First European Conference on Earthquake Engineering and Seismology
(a joint event of the 13th ECEE & 30th General Assembly of the ESC)
Geneva, Switzerland, 3-8 September 2006
Paper Number: 844

NUMERICAL TOOL TO STUDY STRUCTURAL REINFORCEMENT OF STEEL REINFORCED CONCRETE (RC) STRUCTURES UNDER SEISMIC LOADS USING FIBER REINFORCED POLYMERS (FRP)

Xavier MARTINEZ[1], Sergio OLLER[2] and Alex BARBAT[3]

SUMMARY

Strengthening or retrofitting existing structures in order to increase their ductility and improve their seismic response has traditionally been accomplished using conventional materials and construction techniques. Composite materials of a polymeric matrix reinforced with long fibres (FRP) have emerged as an alternative to these methods.
To view the performance of these reinforcements when seismic loads are applied, this work studies the structural response of a frame joint when a horizontal load is applied to it. Under a seismic load, joints are one of the weakest parts of these structures. The response of a plain concrete frame joint is compared with the response obtained when it is reinforced using FRP. Different configurations of FRP reinforcements are considered to compare their behaviour.
The structural response of all structures considered is obtained with a numerical simulation. This is done using the finite element method. Composites are treated using the mixing theory, which obtains the composite behaviour by means of the composition of each component material properties. Each component is simulated with its own constitutive equation. The anisotropy usually found in composite components is treated using a mapped space theory. The debounding effects found in composite materials are treated using the formulation developed by E. Car and S. Oller [Car, 2000].
The results obtained validate the use of FRP reinforcements to improve frames seismic response. The structure load capacity is increased in a 20% when lateral reinforcements are applied to the joint. This can avoid the structure to collapse in a seismic case. They results also show a good performance of the numerical tool developed.

1. INTRODUCTION

Multiple studies have been carried out to obtain the structural performance of FRP reinforced and retrofitted structures and to know how the reinforcement behaves. All these studies use experimental techniques, supported and complemented with analytical calculations.

On the other hand, the study of composite materials has been one of the major objectives of computational mechanics in the last decades. Many theories and simulation procedures have appeared to predict the structural behaviour of composites. Some of the topics in which the studies have been focused are the modelling of composite materials, their structural strength mechanisms and their failure causes.

[1] Universitat Politècnica de Catalunya (UPC). Edificio C1, Campus Nord, UPC. Gran Capità s/n. 08034, Barcelona, Spain
Email : xaviermg@cimne.upc.edu
[2] Universitat Politècnica de Catalunya (UPC). Edificio C1, Campus Nord, UPC. Gran Capità s/n. 08034, Barcelona, Spain
Email: sergio.oller@upc.edu
[3] Universitat Politècnica de Catalunya (UPC). Edificio C1, Campus Nord, UPC. Gran Capità s/n. 08034, Barcelona, Spain
Email: alex.barbat@upc.edu

In despite of all existing studies in both fields: experimental tests of FRP reinforcements and numerical characterization of composite materials, few investigations have been found in which they are coupled. This is, the study of the FRP reinforcement problem using a numerical point of view. Under this scope, this paper presents a finite element code which allows studying the problem of reinforced and retrofitted concrete structures with FRP.

The finite element code is validated using the experimental results corresponding to a RC beam with a carbon fibre reinforced polymer (CFRP) reinforcement to improve its strength to bending. These results have been obtained from [Spadea *et al*., 1998]. The agreement between numerical and experimental results allows using the code for other simulations in which no experimental results are available.

The finite element code will be used to obtain the capacity of fibre reinforced polymers to improve the structural response of reinforced concrete frames to seismic loads. Different CFRP reinforcements will be applied to the frame joint between the beam and the column to study the behaviour of each reinforcement, as well as the global behaviour of the structure.

2. FINITE ELEMENT CODE DESCRIPTION AND VALIDATION

2.1 Code description

Modelling composite materials has been done, traditionally, by using a single orthotropic material with average properties from its different constituents, obtained form experimental results. This method has not provided satisfactory results, mainly when one of the constituents reaches its yield point or when the change of fibre orientation is made in the basic material. To solve this problem, different formulations have appeared recently which allow studying the structure at the level of the composite material, obtaining its behaviour from the characteristics and properties of its constituent materials. These formulations are: Homogenization theory [Zalamea, 2001] and the Rule of Mixtures [Trusdell and Toupin, 1960, Car, 2000 and Rastellini *et al.*, 2003].

The simulation shown in the present paper is done with a 2D/3D finite element code (PLCD) that can deal with kinematics and material nonlinearities. It contains various constitutive laws to predict the material behaviour: Von-Mises, Mohr-Coulomb, improved Mohr-Coulomb, Drucker-Prager, etc. [Malvern, 1996 and Oller, 1988]. It uses different integration algorithms to simulate the material evolution: Elastic, visco-elastic, damage, damage-plasticity, etc. [Oller, 2001]. The analysis performed by PLCD code can be static or dynamic (using the Newmark method, [Oller, 2002]).

The theories and numerical procedures included in PLCD code to simulate composite materials are:

2.1.1 Classic Rule of Mixtures

The classical rule of mixtures was originally developed by Trusdell and Toupin [1960]. It considers that the interaction between the components in a material point of the composite is done according to the following hypothesis: (i) each infinitesimal volume of the composite contains a finite number of material components; (ii) each component contribution to the global behaviour of the composite is proportional to its volumetric participation; (iii) all components suffer the same strains (closing equation); (iv) the volume of each component is significantly smaller than the composite volume.

The third hypothesis, in the case of small strains, can be written as:

$$\varepsilon_{ij} = (\varepsilon_{ij})_1 = (\varepsilon_{ij})_2 = (\varepsilon_{ij})_3 = \ldots = (\varepsilon_{ij})_n \tag{1}$$

Where, ε_{ij} is the strain tensor for the composite and $(\varepsilon_{ij})_n$ is the strain tensor for each component of the composite. According to second hypothesis, the free energy of the composite becomes the addition of the free energies of each component of the composite, weighted by the volumetric participation of the component. This is:

$$m \cdot \psi(\varepsilon^e, \alpha^m) = \sum_{c=1,n} k_c \cdot m_c \cdot \psi_c(\varepsilon, \varepsilon_c^P, \alpha_c^m) \tag{2}$$

In equation (2), m is the mass, ψ the free energy and α^m the internal variables of the composite (when no subscript is displayed) and of each component of the composite (when subscript c is added). The strains ε, ε^e and ε^p correspond to the total strain, the elastic strain and the plastic strain respectively. Parameter k_c is the volumetric participation of each component in the composite, defined as:

$$k_c = \frac{dV_c}{dV_0} \tag{3}$$

The constitutive equation can be obtained applying Coleman's method to the Clasius-Duhem inequality [Oller *et al.*, 1996]:

$$\sigma_{ij} = m \cdot \frac{\partial \psi(\varepsilon_{ij}; \alpha_i)}{\partial \varepsilon_{ij}} = \sum_{c=1,n} k_c \cdot m_c \cdot \frac{\partial \psi_c(\varepsilon_{ij}; \alpha_i)}{\partial \varepsilon_{ij}} = \sum_{c=1,n} k_c \cdot (\sigma_{ij})_c = \sum_{c=1,n} k_c \cdot (C^S_{ijkl})_c \cdot (\varepsilon^e_{ij})_c \tag{4}$$

Where $(C^S_{ijkl})_c$ is the secant constitutive tensor.

Equation (4) shows that the composite performance is obtained as a proportional average of its constituent materials response to a strain state, defining each constituent material with its own constitutive law. The numerical implementation of this theory in a F.E.M code is shown in Figure 1. A more detailed explanation of this implementation, as well as the extension to the large deformations case, can be found in [Car, 2000]

2.1.2 Anisotropy using a mapping space theory

This theory is based on the transport of all the constitutive parameters and the stress and strain states of the structure, from a real anisotropic space to a fictitious isotropic space. Once all variables are in the fictitious isotropic space, an isotropic constitutive model can be used to obtain the new structure configuration. This theory allows considering materials with high anisotropy, such as composite materials, using all the techniques and procedures already developed for isotropic materials.

All the anisotropy information is contained in a fourth order tensor. This tensor relates the stresses and the strains in the fictitious isotropic space to the stresses and the strains in the real anisotropic space according to equations (5) and (6), respectively.

$$\overline{\sigma_{ij}} = A^{\sigma}_{ijkl} \cdot \sigma_{ij} \tag{5}$$

$$\overline{\varepsilon_{ij}} = A^{\varepsilon}_{ijkl} \cdot \varepsilon^e_{ij} \tag{6}$$

A representation of these transformations is displayed in Figure 2. A more detailed description of this methodology, the extension to large strains and its numerical implementation can be obtained in [Car *et al.,* 2001 and Car, 2000]

2.1.3 Fibre-matrix debounding

The apparition of matrix cracks in a composite material is usually followed by a relative movement between the fibres and the matrix. This lost of adherence implies a stiffness reduction in the composite material. This phenomenon is introduced in the elastic limit of the material as a modification of its yield surface criterion. The new fibre elastic limit becomes:

$$(f^R)_{fib} = \min\left\{ (f^N)_{fib};\ (f^N)_{mat};\ \left[2 \cdot (f^N)_{fib-mat} / r_{fib} \right] \right\} \tag{7}$$

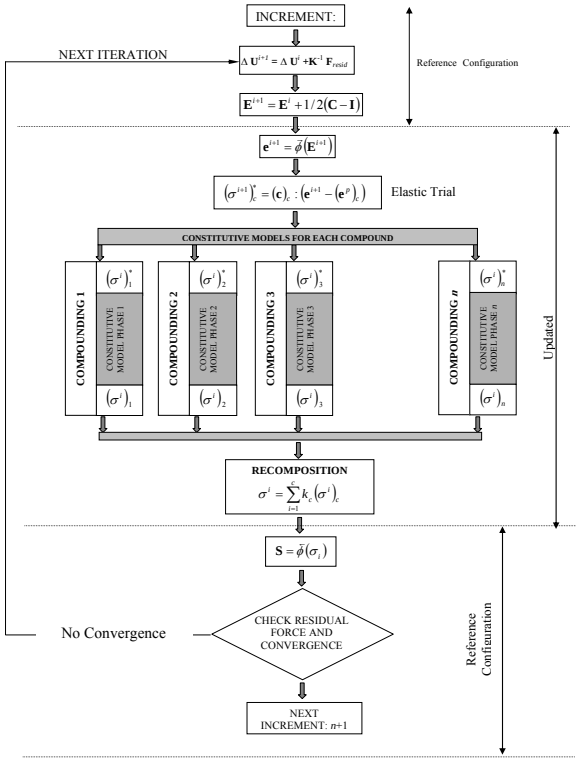

Figure 1: Implementation of the Rule of Mixtures in a finite element code (image obtained from [Car et al., 2000])

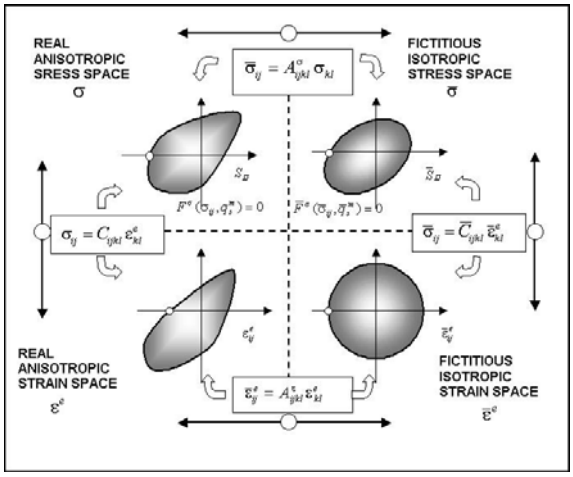

Figure 2: Space transformations. Real and fictitious stress and strain spaces in small strain (image obtained form [Car et al., 2001])

Where $(f^R)_{fib}$ is the new fibre strength, $(f^N)_{fib}$ is the nominal fibre strength, $(f^N)_{mat}$ is the matrix nominal strength and $(f^N)_{fib-mat}$ is the fibre-matrix interface nominal strength. Equation (7) shows that the debounding happens when one of the composite constituents reaches its nominal strength (considering the fibre-matrix interface as a constituent). The nominal resistance values are obtained from the material properties. The numerical implementation of this phenomenon is described in [Car, 2000 and Oller, 2002]

2.1.4 Construction Stages Algorithm

Retrofit a structure implies the addition of the structural reinforcement once the original structure is already damaged. The *"Construction Stages Algorithm"* implemented in PLCD permits running the numerical simulation during the desired load cases, with only some structural elements active on the structure. At a certain load case, new elements can be added without stopping the calculation process. These new elements are free of strains and stresses when they are activated.

The algorithm requires having all elements defined in the structure. The elastic strains are divided in two components, and active and a non-active (equation (8)). If the element is not present in the structure, all strains correspond to the non-active part (equation (9)) while, if the element is active, all strains corresponding to the non-active situation will be removed (equation (10)) from the total strain. Stresses are computed considering only the active elements (equation (11))

$$\varepsilon^e = \varepsilon^e_A + \varepsilon^e_{NA} \tag{8}$$

$$\varepsilon^e_{NA} = \varepsilon^e; \qquad \varepsilon^e_A = 0 \tag{9}$$

$$\varepsilon^e_A = \varepsilon^e - \varepsilon^e_{NA} \tag{10}$$

$$\sigma^e = C^e \cdot \varepsilon^e_A \tag{11}$$

With this procedure, to avoid the non-active elements to contribute to the global stiffness, their constitutive tensor has to be nullified at the beginning of the construction stage, when the global stiffness matrix is generated.

2.2 Finite element code validation

The code ability to predict the behaviour of a structure reinforced with CFRP is tested using the experimental results reported by G. Spadea [Spadea *et al.*, 1998]. In this paper, the reinforced concrete beam shown in Figure 3 is reinforced using different CFRP reinforcement configurations. The configuration chosen to do the code validation corresponds to the bending reinforced beam and to the beam without reinforcement.

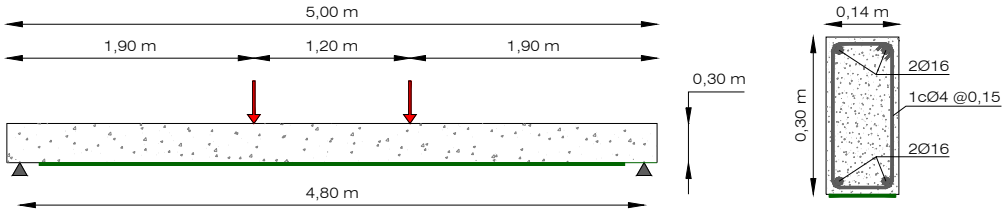

Figure 3: Geometric definition of the beam studied. In green is represented the CFRP reinforcement.

The comparison between the experimental and the numerical results is done using a force-displacement graph (Figure 4). In it, the force applied on the beam is plotted against the displacement of the point where the force is applied. The non reinforced beam shows a larger stiffness in the numerical model, even the beam strength is the same. The curves for the CFRP reinforced beam are practically the same for the numerical and the experimental results. Thus, it can be concluded that PLCD code works properly and is able to simulate with enough accuracy this sort of structures.

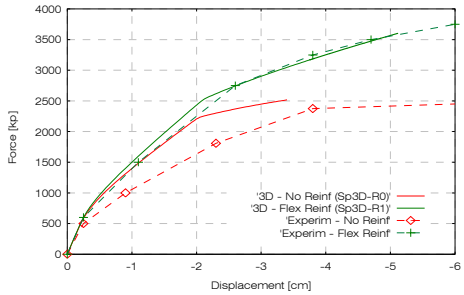

Figure 4: Code validation. Comparison between numerical and experimental results.

3. FRP REINFORCEMENT AND RETROFITTING OF CONCRETE FRAMES

3.1 Joint reinforcement of a steel reinforced concrete frame

Concrete frames are a common used typology in building and civil engineering. One of the most stressed zones of this sort of structures is the connecting joint between the beam and the column. There is many times in which this joint presents a lack of resistance to seismic loads (as a result of a bad design or because the action was not considered). A possible way to increase the frame strength and ductility is by reinforcing the frame joint with CFRP.

Different numerical models have been developed with different CFRP configurations, in order to see the ability of these reinforcements to increase the frame strength and to find which configuration provides better results.

3.1.1 Model description

The concrete fame defined has the geometry and the steel reinforcement commonly found in edification. Figure 5a shows the geometry considered, Figure 5b shows the steel reinforcement of the frame and Figure 5c shows the CFRP reinforcement that will be applied to it. The beam section, as well as its steel reinforcement is under-dimensioned in order to increase the effects of the CFRP reinforcements in the frame joint. The CFRP

reinforcements are composed by layers of unidirectional carbon fibres (66% of the composite volume) embedded in a polymeric matrix (34%); the thickness of each layer is 1,2 mm.

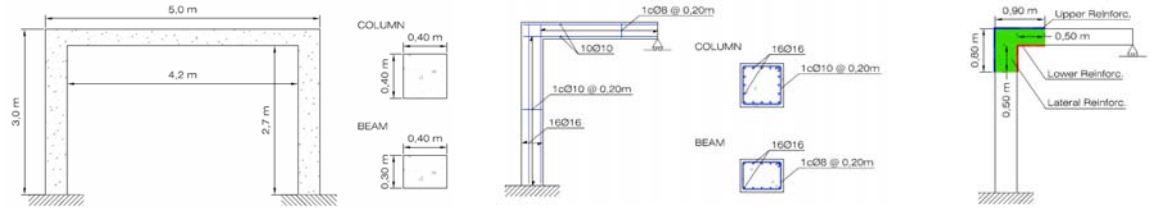

(a) (b) (c)

Figure 5: Geometric definition (a), steel reinforcement (b) and CFRP reinforcement (c) applied to the concrete frame studied

Three different 3D models have been developed. Each model has a different CFRP reinforcement configuration. These are:

- 3D-noR: Concrete frame without CFRP reinforcement
- 3D-R: Concrete frame with the upper and lower CFRP reinforcements
- 3D-LR: Concrete frame with the upper, lower and lateral CFRP reinforcements.

The finite elements corresponding to each CFRP reinforcement layer are added or removed depending in the problem to be computed. The distribution of the different composite materials is displayed in Figure 6.

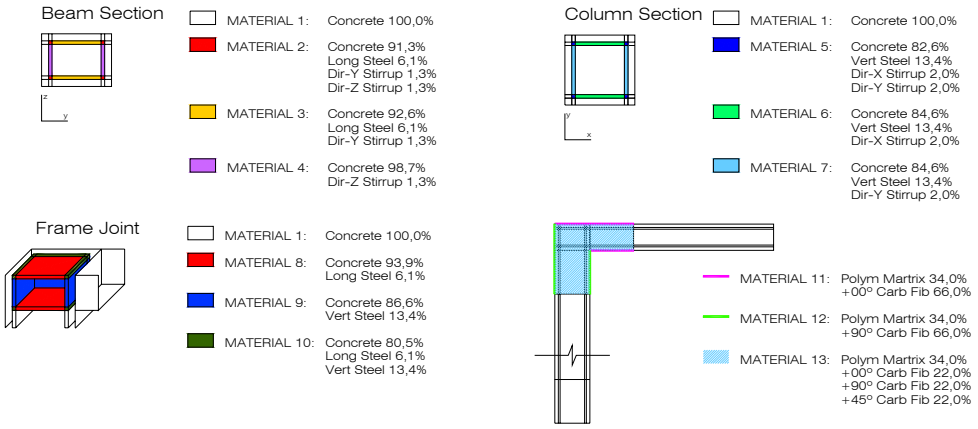

Figure 6: Composite materials distribution in 3D model (3D-LR)

All models use the rule of mixtures to define the composite materials. The mechanical characteristics of the different constituent materials used to generate each composite are described in Table 1. The value of the Young Modulus in the transversal direction has been reduced in fibrous materials (steel and carbon fibres) to force their unidirectional behaviour.

Table 1: Mechanical characteristics of the constituent materials defined in the concrete frame

Material	Yielding criterion	E_{xx} [MPa]	$E_{yy}=E_{zz}$ [MPa]	ν	σ_C [MPa]	σ_T [MPa]	G_C [kPa·m]	G_T [kPa·m]
Concrete	Mohr-Coulomb	$2.5 \cdot 10^4$	$2.5 \cdot 10^4$	0,20	30,0	3,0	50,0	0,5
Steel	Von-Mises	$2,1 \cdot 10^5$	21	0,00	270,0	270,0	2000	2000
Polymeric matrix	Mohr-Coulomb	$1,2 \cdot 10^4$	$1,2 \cdot 10^4$	0,20	87,5	29,2	36,0	3,0
Carbon fibres	Von-Mises	$1,5 \cdot 10^5$	15,2	0,00	2300	2300	2000	2000

Nevertheless the aim of this calculation is obtaining the CFRP reinforcement effect when seismic loads are applied to the concrete frame, a static numerical simulation is performed. A horizontal force, applied in the middle of the frame joint, reproduces the efforts of a seismic load in the structure. This force is applied until the frame ultimate strength, in order to obtain its fracture energy.

3.1.2 Structural behaviour of the different reinforcements applied

The failure criterion of the frame under study, when no reinforcement is applied, is a tensile crack in the beam section beside the joint due to bending forces. This is shown in Figure 7, where the plastic damage variable in concrete is represented (plastic damage values are in between 0,0 (no damage) and 1,0 (full damage). This kind of failure justifies the CFRP reinforcement designed for the structure.

The structural behaviour of the frame joint, for the different CFRP reinforcements applied, is studied using a force-displacement plot (Figure 8). The displacement considered corresponds to the horizontal displacement suffered by the point where the load is applied. This displacement depends on the column, beam and joint stiffness. As the column and the beam are not modified in the different reinforcement models, if the joint stiffness is increased, the force-displacement graph will show this increment.

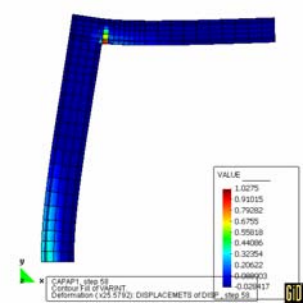

Figure 7: Plastic damage in concrete frame (3D-noR model) when failure occurs.

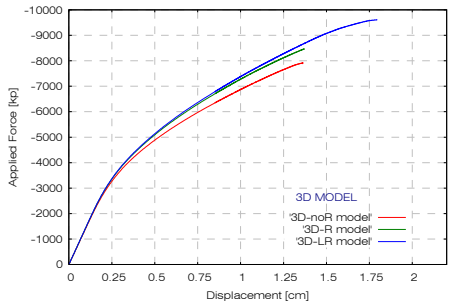

Figure 8: Force-displacement plots obtained with the different models of the concrete frame.

Figure 8 shows that the upper and lower CFRP reinforcements increase the joint stiffness but do not improve significantly the structural strength (the improvement is less than a 9%). On the other hand, when the lateral reinforcement is applied, the frame resistance is increased nearly a 20%.

A better understanding of the results shown in previous plot is obtained by looking at the failure causes on each model. The exact place where the concrete failure occurs in the frame without CFRP reinforcement is displayed in Figure 7. Figure 9 shows plastic damage in concrete when the upper and lower CFRP reinforcements are applied to the frame joint. In this last case, the fracture moves to the inner section of the joint, beside the end of the reinforcement layer. This explains the small resistance increment found with this kind of reinforcement; the failure is exactly the same and nearly in the same place as when no CFRP is applied.

When the lateral CFRP reinforcement is applied to the frame joint (3D-LR model), Figure 8 shows a better performance of the whole structure. This is because lateral reinforcement avoids failure damage in concrete external section (Figure 10.a). Even though, if the whole joint is examined (Figure 10.b), it can be seen that the structure failure still happens in the joint, in its internal sections where no reinforcement is applied. So, even the lateral reinforcement improves the frame joint strength, this improvement is limited to the places where the CFRP can be applied.

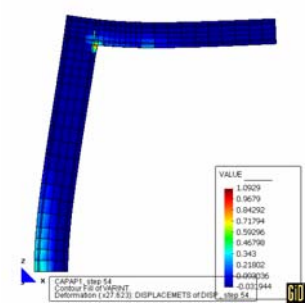

Figure 9: 3D-R model. Plastic damage in concrete when frame failure occurs. Central section.

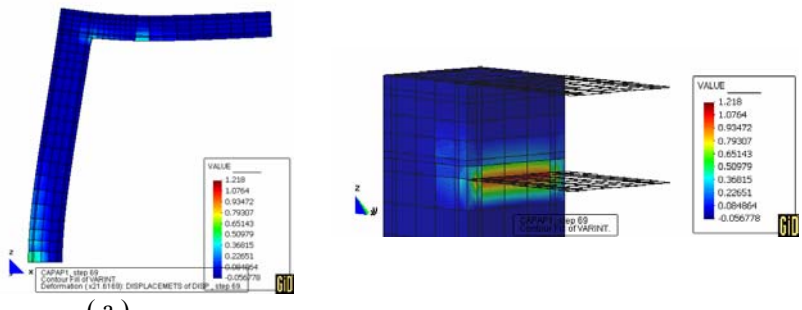

(a) (b)

Figure 10: 3D-LR model. Concrete plastic damage when frame failure occurs. (a) External section. (b) Joint internal section

The maximum stress found in the reinforcement carbon fibres (Table 2) is below the 20% of its yield stress (the stresses shown in the table have been obtained from the 3D-LR model). So, even the CFRP reinforcement increase the frame resistance, the structure cannot transfer to it enough stresses to obtain a major improvement.

Table 2: Maximum stress in reinforcements carbon fibres (3D-LR model)

Reinforcement	Fibre orientation	Stress [kp/cm²]
Upper	+ 0º	- 1407,4
	+ 90º	- 430,2
Lower	+ 0º	+ 4687,0
	+ 90º	+ 1727,7
Lateral	+ 0º	+ 4687,0
	+ 90º	+ 1727,7
	+ 45º	+ 1165,8

3.1.3 Lateral FRP reinforcement configurations

As lateral CFRP reinforcement is the one that provides better results, three different configurations have been tested to obtain the most suitable reinforcement scheme. These simulations have been done with two dimensional models (which provide worst results but require less computational effort). The lateral CFRP reinforcements defined are:

- 2D-LR-1: Lateral reinforcement with three layers of carbon fibres, oriented at 0º, +90º and +45 (counter clockwise) respect the horizontal.
- 2D-LR-2: Lateral reinforcement two layers of carbon fibres, oriented at 0º and 90º respect the horizontal.
- 2D-LR-3: Lateral reinforcement with a single layer of carbon fibres, oriented at +45º (contraclockwise) respect the horizontal.

The force-displacement graph (Figure 11.a) does not show any remarkable difference among the different lateral reinforcements applied to the structure. Even though, analyzing the evolution of the angle defined by the beam and the column (Figure 11.b), a different performance is observed for each model.

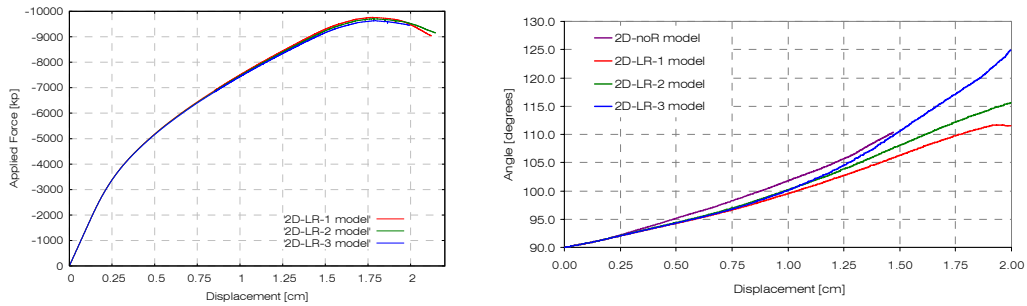

(a) (b)

Figure 11: Graphs with (a) force-displacement and (b) frame angle-displacement for the different lateral reinforcement models

For small deformations of the frame joint, all lateral reinforcements present a similar behaviour. But, as the joint increases its deformation, the reinforcement that only contains fibres at +45º (2D-RL-3 model) does not provide strength enough to the frame joint and its angle opens as when no reinforcement is applied to the frame joint.

The frame joint in 2D-LR-1 and 2D-LR-2 models are stiffer than the joint in model 2D-LR-3, due to the presence of longitudinal carbon fibres. The principal stress in the joint angle (point A, Figure 12) has a direction of +45º. When horizontal and vertical carbon fibres are included in the reinforcement, the resultant stress corresponds to the same stress found when the reinforcement only has fibres oriented at +45º, plus a horizontal component that gives the joint additional stiffness.

Table 3 shows the carbon fibre stresses at point A in models 2D-LR-2 and 2D-LR-3. The composition of stresses is developed below. The stresses in +45º direction are practically the same for both models. Fibres in model 2D-LR-2 develop an additional a stress in their horizontal direction that gives the additional stiffness to the structure.

Thus, it can be concluded that fibres oriented at +45º restrain the crack effects in the joint angle while fibres oriented at 0º offer an additional stiffness to the structure.

Table 3: Stresses in lateral reinforcement carbon fibres. 2D-LR-1 and 2D-LR-3 models

Model	Stresses	+0º carbon fibres	+90º carbon fibres	+45º carbon fibres
2D-LR-2	Sxx [kp/cm²]	4660.7		
	Syy [kp/cm²]		1644.1	
2D-LR-3	Sxx [kp/cm²]			1747.9
	Syy [kp/cm²]			1749.0

Composition of stresses in 2D-LR-2 model:

$\sigma_{+0º}$ = 3016,6 kp / cm^2

$\sigma_{+45º}$ = 2325,1 kp / cm^2

Composition of stresses in 2D-LR-3 model:

$\sigma_{+45º}$ = 2472,7 kp / cm^2

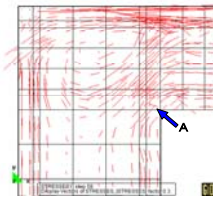

Figure 12: Principal stresses direction

3.2 Bending retrofitting of a reinforced concrete beam

The behaviour of CFRP reinforcements when they are applied to a structure which is already damaged is studied using the beam described in the code validation. Two different retrofit cases have been considered according to the moment in which the reinforcement is applied. Both models will be compared with a bending CFRP reinforced beam (Sp3D-R1) which has the reinforcement from the beginning of the load process, and with a beam without CFRP reinforcement (Sp3D-R0). The models defined are:

- Sp3D-Rt2: Bending CFRP retrofitted beam. The reinforcement is applied just before the concrete reaches its yield limit stress.
- Sp3D-R3: Bending CFRP retrofitted beam. The reinforcement is applied just before the longitudinal steel reaches its yield limit stress.

3.2.1 Results obtained

The comparison among the results obtained with the reinforced and the retrofitted beams models is done with a force-displacement graph (Figure 13). This graph shows that the structural stiffness does not depend on when the reinforcement is applied. The structure stiffness obtained when the CFRP reinforcement is applied after steel yielding (Sp3D-Rt3 model) does not differ significantly from the structure stiffness obtained after the steel yielding in the reinforced model (Sp3D-R1).

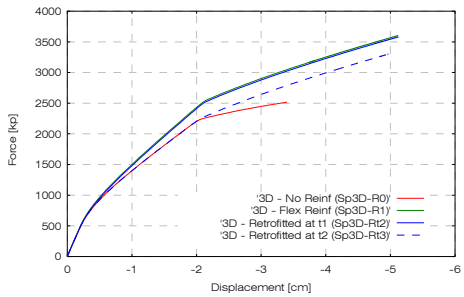

Figure 13: Comparison between flexion CFRP reinforced and retrofitted three dimensional beams

On the other hand, to retrofit a structure implies that, when the CFRP reinforcement starts collaborating, the structure will have a deformation and damage larger than if it had been reinforced from the beginning. Damage will reduce the load capacity of the beam while deformation can make the serviceability state unacceptable (i.e. when a load of 3000 kp is applied to the structure, the beam deformations are 23% larger in the retrofit model, Sp3D-Rt3, than in the reinforced one, Sp3D-R1).

4. CONCLUSIONS

The numerical simulation realized in the present paper shows that CFRP reinforcements applied to the joint between the beam and the column can improve considerably the strength capacity of reinforced concrete frames. Even though, this increment depends on how this reinforcement is applied. If only upper and lower reinforcements are attached to the frame joint, the load capacity is increased in a 9%, while if lateral reinforcements are also applied, this increment reaches a 20%.

Even the strength improvement justify the use of CFRP reinforcements, their behaviour is not efficient. As reinforcements are attached to the surface of the frame joint, they cannot reinforce its interior: the failure section moves from the outer section to the inner one, but still happens in the frame joint. Besides, the carbon fibres cannot develop their whole strength capacity (their largest stress does not reach the 20% of the yielding stress).

The comparison between the results obtained with CFRP reinforcement and retrofitting shows that the structure stiffness does not vary significantly. Although, later the reinforcement is applied, more deformed will be the structure and lower will be its load capacity. So, if the structure serviceability is conditioned by the deformations, the CFRP reinforcement should be applied as soon as possible.

The finite element code developed is a good tool to simulate CFRP reinforcements and retrofittings of RC structures. Allowing different numerical simulations with different CFRP reinforcements to obtain the most suitable solution for the problem under study, reducing the times and costs required if the same simulation has to be done in a laboratory.

5. ACKNOWLEDGEMENTS

This work has been supported by C.E.E.-FP6 (LESSLOSS project, Ref. FP6-505448(GOCE)); Ministerio de Fomento and Ministerio de Ciencia y Tecnología (DECOMAR project, Ref. MAT-2003-09768-C03-02).

6. REFERENCES

Car, E., Oller, S., Oñate, E. (2000) An anisotropic elastoplastic constitutive model for large strain
analysis of fiber reinforced composite materials, *Computer methods in applied mechanics and engineering,* 185, nº 2-4, 245-277

Car, E. (2000), Modelo constitutivo continuo para el estudio del comportamiento mecánico de los materiales compuestos, *PhD Thesis, Departament de Resistència de Materials i Estructures a l'Enginyeria (RMEE)*, Politechnical University of Catalonia (UPC), Spain.

Car, E., Oller, S., Oñate, E. (2001), A large strain plasticity model for anisotropic materials – composite material application, *International Journal of Plasticity*, 17, nº. 11, 1437-463.

Malvern, L. E. (1968), Introduction to the mechanics of a continuous medium, *Prentice-Hall*, Englewood Cliffs, NJ, USA.

Oller, S. (1988), Un modelo de daño continuo para materials friccionales, *PhD Thesis, (RMEE)*, Politechnical University of Catalonia (UPC), Spain.

Oller, S., Oñate, E., Miquel, J., Botello, S. (1996), A plastic damage constitutive model for composite materials, *International Journal Solids and Structures*, 33, nº17, 2501-2518

Oller, S. (2001), Fractura mecánica. Un enfoque global, *CIMNE*, Barcelona, Spain

Oller, S. (2002), Análisis y cálculo de estructuras de materiales compuestos, *CIMNE,* Barcelona, Spain

Oller, S. (2002), Dinámica no-lineal, monograph M63, *CIMNE*, Barcelona, Spain

Rastellini, F., Oller, S., Salomon, O., Oñate E. (2003), Advanced serial-parallel mixing theory for composite materials analysis. Continuum basis and finite element applicantons, *Proceedings CD of the VII International Conference on Computational Plasticity COMPLASS 2003*, CIMNE, Barcelona, Spain.

Spadea, G., Benicardino, F., Swamy, R.N. (1998) Structural behaviour of composite RC beams with externally bonded CFRP, *Journal of Composites for Construction*; 2, nº 3, 132-137.

Trusdell, C., Toupin, R. (1960), The Classical Field Theories, Handbuch der Physik III/I, *Springer Verlag*, Berlin, Germany.

Zalamea, F. (2001), Tratamiento numérico de materiales compuestos mediante la teoría de homogeneización, *Ph.D. thesis, Departament de Resistència de Materials i Estructures a l'Enginyeria (RMEE)*, Politechnical University of Catalonia (UPC), Spain.